

Observation of densely populated Tamm states in modulation-doped superlattices

A. B. Henriques and L. K. Hanamoto

Instituto de Física, Universidade de São Paulo, Caixa Postal 66318, 05315-970 São Paulo, Brazil

P. L. Souza and B. Yavich

Centro de Estudos em Telecomunicações, Pontifícia Universidade Católica, Rua Marques de São Vicente, 225, 22453-900 Rio de Janeiro, Brazil

(Received 3 December 1999; revised manuscript received 10 January 2000)

We have observed densely populated surface-localized states (Tamm states) in doped lattice-matched $\text{InP}/\text{In}_x\text{Ga}_{1-x}\text{As}$ superlattices. The formation of Tamm states is manifested in the Shubnikov–de Haas (SdH) spectra in tilted magnetic fields. Along with SdH oscillations due to quasi-three-dimensional (3D) carriers, which fill a superlattice miniband, SdH oscillations due to 2D carriers are seen. The 2D subband has an energy threshold greater than the superlattice miniband, and it is associated with surface-localized states. Cyclotron mass measurements and theoretical calculations of the electronic energy levels provide support for the interpretation. The role of the surface-localized states in the transport properties of the superlattice is also investigated.

I. INTRODUCTION

Because of their finite size, even perfect crystals may have energy levels within the energy gaps between the allowed bands of energies of an ideal infinite crystal. The wave functions associated with these energy levels are localized at the surfaces. Such states were first described by Tamm¹ and are known as “Tamm states,” or surface states. At real surfaces, the observation of pure Tamm states is difficult because of the complicated nature of the surfaces, where many effects operate concurrently, leading to a single-particle potential that is difficult to control and engineer. Superlattices, on the other hand, provide an ideal platform in which to study the effects of the surface upon the electronic properties of solids, since precise control over the confining potential at the boundaries of the superlattice material (the so-called “internal surface”) is possible. Tamm states in undoped superlattices have been studied experimentally^{2–5} and theoretically.^{6–11} The origin of the surface states can be understood from a tight-binding approach. Whereas the subband energy levels develop into a miniband when the coupling between wells is switched on, the subband levels of the outer wells may remain nonresonant with the rest and contain localized states. Imposing some sort of perturbation upon the system can be used to control the detachment in energy of the outer wells, to produce surface-localized states. Several perturbations near the internal surface have been attempted, such as different barrier height at the end than the rest of the potential barriers in the superlattice,^{2,8,9,7} a different well width,³ a δ defect,¹¹ etc. Indeed, it was in a perturbed undoped superlattice that Tamm states were first observed,^{2,4} but much less attention has been paid to doped superlattices. In this paper we demonstrate that in doped superlattices Tamm states exist even if no intentional perturbation near the surface is employed. Moreover, in doped superlattices Tamm states can be densely populated with electrons, and we report their observation. The populated Tamm states can affect the transport properties, which has

both fundamental and practical importance, and so we also investigate this aspect.

We studied lattice-matched $\text{In}_x\text{Ga}_{1-x}\text{As}/\text{InP}$ modulation-doped superlattices. The presence of Tamm states was detected through Shubnikov–de Haas (SdH) spectra. In addition to a beating oscillatory magnetoresistance, an oscillatory component was detected at lower frequencies. The source for these oscillations was deduced from their behavior when the magnetic field was tilted relative to the axis of the superlattice. The beating magneto-oscillatory component showed a behavior typical of quasi-three-dimensional carriers filling a superlattice miniband, whereas the component at lower frequencies is characteristic of electrons in two dimensions (2D). The cyclotron mass of the 2D electrons was deduced from the thermal dependence of the SdH oscillations, and the value obtained shows that the 2D electrons are located in an $\text{In}_x\text{Ga}_{1-x}\text{As}$ layer. On the basis of a theoretical model for the electronic energy levels in the superlattices, we demonstrate that the 2D electrons belong to a Tamm state. The existence of Tamm states in modulation-doped superlattices is a direct consequence of the inhomogeneous space charge present in these systems, which causes bending of the energy bands near the boundaries of the superlattice.

II. EXPERIMENTAL

The superlattice structures, grown by low pressure metal-organic vapor phase epitaxy (LP-MOVPE), consisted of 16 $\text{In}_x\text{Ga}_{1-x}\text{As}$ wells of 50-Å width, separated by 15 InP barriers. All InP barriers were δ doped with Si atoms at their center with a doping density about $4 \times 10^{12} \text{ cm}^{-2}$. The samples were grown on a 75-nm-thick undoped InP buffer layer deposited on a semi-insulating InP substrate, and terminated with 30-nm undoped InP cap layer. X-ray diffraction was used to deduce the period of the structures. More details on the growth procedure and on the structural characterization of the samples are given in Ref. 12. Here we report measurements on two samples: No. 326, in which the thickness of the InP barriers is a 50 Å barrier, and No. 331,

TABLE I. Parameters of the samples studied. The Hall density, n_H , and mobility, μ_H , were measured at 4.2 K. The sheet carrier density per period, n_S , and the fundamental miniband width, Δ_{E1} , were deduced from the theoretical calculations.

Sample	InP barrier thickness (\AA)	n_H (cm^{-2})	μ_H (cm^{-2}/Vs)	n_S (cm^{-2})	Δ_{E1} (meV)
326	50	3.3×10^{12}	6440	3.4×10^{12}	23.2
331	40	3.4×10^{12}	5460	3.6×10^{12}	36.3

in which the thickness of InP barriers is 40 \AA . SdH spectra were measured using an 18 T superconducting magnet with a variable temperature insert. The sample holder had a gear mechanism which allowed the adjustment of the tilt angle θ (the angle between the magnetic field direction and the axis of the superlattice) with an accuracy of about $\pm 2^\circ$. The SdH data were expressed in reciprocal magnetic field, numerically differentiated to suppress the monotonic background, and frequency analyzed by Fourier techniques. Low magnetic field measurements of the Hall carrier concentration, n_H , and Hall mobility, μ_H , were also performed at 4.2 K.

III. RESULTS AND DISCUSSION

The results of the Hall measurements are given in Table I for both samples studied.

Figures 1(a) and 1(c) show the SdH spectra for the samples as a function of the tilt angle. To reveal the dimensionality of the carriers responsible for the SdH oscillations, the Fourier amplitude was plotted against the *reduced* Fourier frequency (the product of the frequency and the cosine of the tilt angle). Since 2D electrons only respond to the magnetic field component normal to the plane of confinement, such a plot for 2D electrons will be independent of the tilt angle. However, due to the limited magnetic field intensity that can be reached (18 T in our experiments), the amplitude of the Fourier peak will decrease with increasing θ , implying that the Fourier spectra become noisier. Figures 1(b) and 1(d) show the Fourier amplitudes plotted against reduced frequency for the SdH spectra of Fig. 1(a) and Fig. 1(c), respectively. In Fig. 1 all Fourier curves were normalized to the same height. The spectra show a peak around 35 T, which is independent of the tilt angle, demonstrating the presence of 2D carriers in the samples. At higher reduced frequencies a doublet structure is seen, whose mean is approximately independent of the tilt angle, but the separation between the two peaks comprising the doublet oscillates with θ . This behavior is typical of carriers belonging to a superlattice miniband described by a Fermi surface with the shape of a corrugated cylinder, with a cross-sectional area modulated along the k_z direction.¹³ For $\theta=0$, two extremal cyclotron orbits perpendicular to the magnetic field direction, a ‘belly’ and a ‘neck,’ contribute with separate frequencies to the SdH oscillations. When θ is increased, the mean k -space area enclosed by both extremal orbits increases roughly as $\sim 1/\cos \theta$, but at certain tilt angles the extremal areas collapse into a single value,¹⁴ and only a single SdH frequency can be observed.

The peak positions in the Fourier spectra in Figs. 1(b),(d) are plotted in Fig. 2. The full curves in Fig. 2 were calculated by solving the Schrödinger and Poisson equations self-

consistently for an infinite superlattice, i.e., the single-particle confining potential for electrons was assumed periodic and the Bloch theorem was used.¹⁵ The carrier and dopant densities were assumed equal and used as an adjustable parameter to fit the experimental peak frequency values of the doublet structure described above. The carrier density obtained is given in Table I. The best fit, shown by full

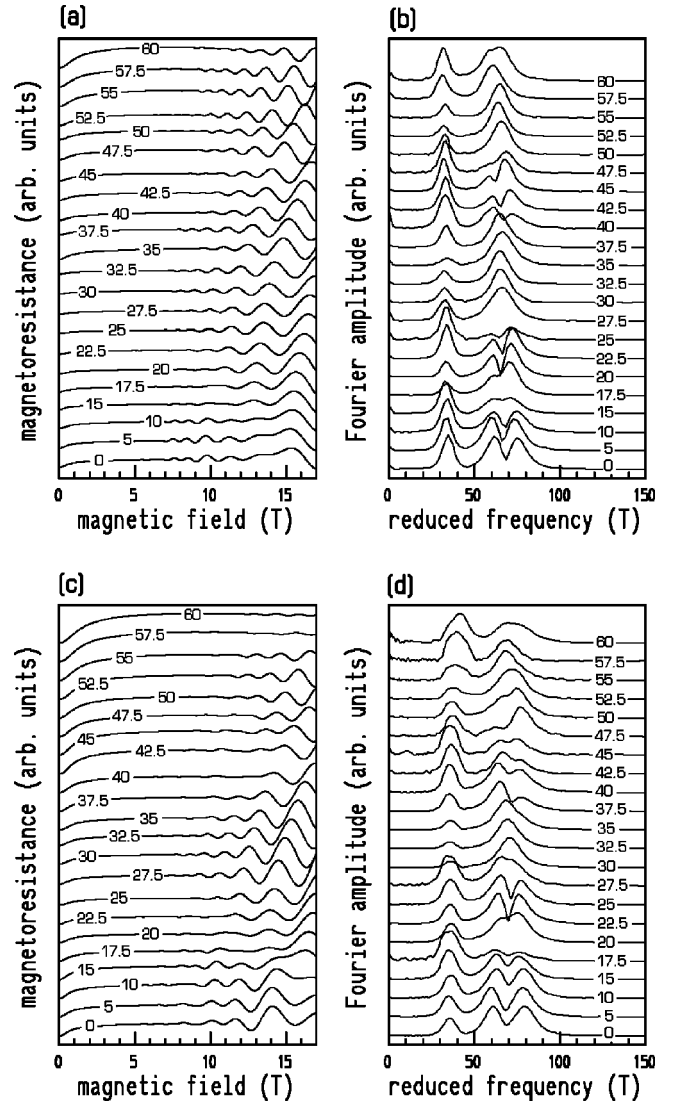


FIG. 1. (a) Angle dependence of the Shubnikov–de Haas spectrum for sample 326. The tilt angle corresponding to each curve is indicated. (b) Reduced frequency plot of the Fourier transform of the oscillations shown in (a). (c) same as (a) but for sample 331. (d) Reduced frequency plot of the Fourier transform of the oscillations shown in (c).

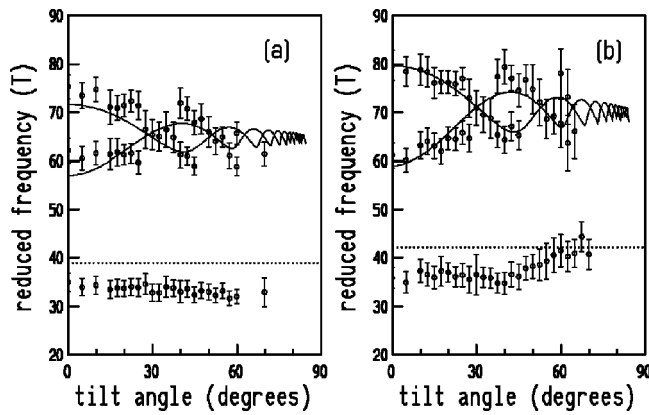


FIG. 2. (a) Angle dependence of the peak positions detected in the reduced frequency plot of the Fourier transform of the SdH oscillations for sample 326. The height of the error bars is equal to the halfwidth of the Fourier bands. Solid lines are theoretical values for the infinite superlattice model. Dotted line is the theoretical value for the contribution from surface-localized electrons, as deduced from a theory for the finite superlattice. (b) Same as in (a) but for sample 331.

curves in Figs. 2(a) and 2(b), is in good agreement with the experimental values, demonstrating that the doublet structure is associated with carriers characteristic of an infinite superlattice. The calculations also yielded the energy width of the fundamental miniband (given in Table I) and show that the miniband dispersion in sample 331 is greater than in sample 326; this is due to the narrower InP barrier in the former.

However, the infinite superlattice model does not predict the SdH oscillations of frequency about 35T [see Figs. 1(b) and 1(d)] for both samples, which is due to 2D carriers. To provide support for the hypothesis that the 2D carriers occupy a surface-localized state, their cyclotron mass was estimated from the temperature dependence of the SdH oscillations at $\theta=0$. For both samples, the cyclotron mass obtained is 0.057 ± 0.0005 in units of the free electron mass. This value is typical of electrons confined in 40–50 Å $\text{In}_x\text{Ga}_{1-x}\text{As}/\text{InP}$ quantum wells,¹⁶ showing that in our samples the 2D electrons are localized mostly in an $\text{In}_x\text{Ga}_{1-x}\text{As}$ layer.

The Schrödinger and Poisson equations were also solved for a superlattice containing a finite number of periods, using the same number of layers and layer widths as the real samples, and also using the carrier density estimated from the infinite superlattice model (see Table I). Figure 3(a) shows the self-consistent potential profile obtained and Fig. 3(b) shows the associated density of states (full line) for sample No. 326. In both figures the origin of the energy scale was chosen at the Fermi level. Also depicted in Fig. 3(b) is the density of states calculated for the infinite superlattice (dashed line). The fundamental miniband dispersion and its population in both models are in approximate agreement. However, for the finite superlattice a localized state appears, at an energy about halfway between the fundamental and the excited miniband, but well below the Fermi level. The envelope wave function associated with this midgap state, plotted in Fig. 3(a) by the thick curve, describes electrons that are localized in the $\text{In}_x\text{Ga}_{1-x}\text{As}$ layers at the edges of the superlattice. This is consistent with the measured value of the cyclotron mass of the 2D carriers, which locates them in an

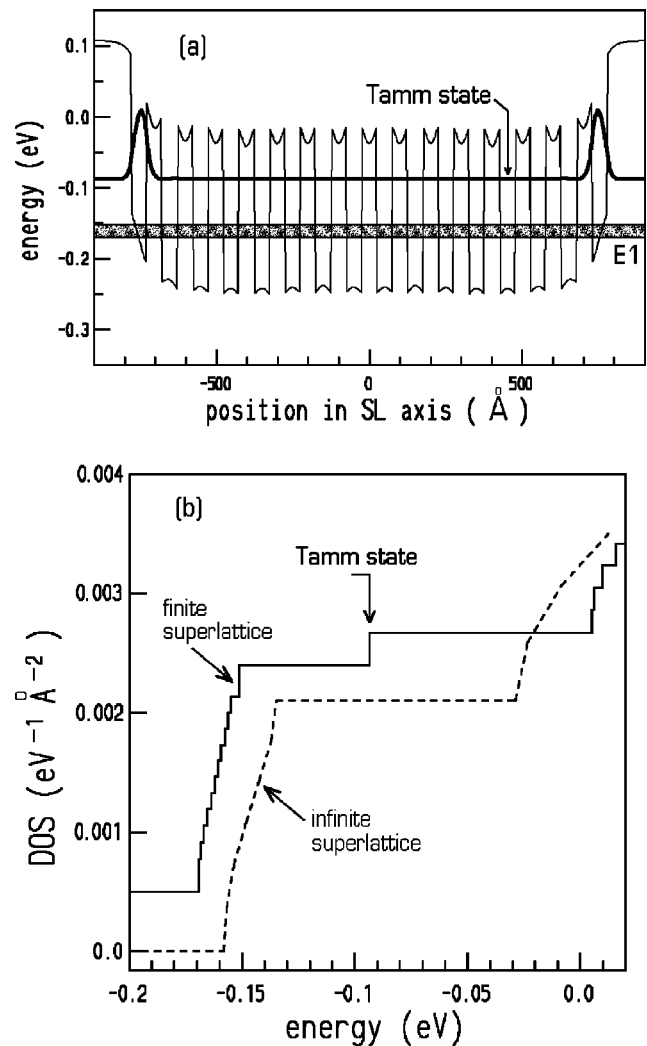


FIG. 3. (a) Self-consistent potential for sample 326. Fundamental miniband $E1$ is indicated by the shaded area. The thick line shows the charge distribution in the Tamm states. (b) Density of states (DOS) in the superlattice. Dashed line is the DOS obtained from the infinite superlattice model. Full line represents DOS for the finite superlattice; this curve was displaced vertically for clarity. The step in the DOS at the energy of the Tamm state is indicated.

$\text{In}_x\text{Ga}_{1-x}\text{As}$ layer. The finite superlattice model also yielded the theoretical frequency of magnetoresistance oscillations associated with the electrons in the Tamm state in both samples, shown in Fig. 2 by the dashed lines, which agree approximately with the experimental values. The small discrepancy between theory and experiment could be due to effects of nonparabolicity and interface nonabruptness, factors that were not taken into account in the calculations.

The Tamm states in doped superlattices arise because of the energy band bending effect, which raises the wells at the edges of the finite superlattice above the rest of the wells, as can be seen in Fig. 3(a). The amount to which the wells at the edges are raised depends on the doping level. For an intrinsic superlattice, no localized state exists. With increasing doping the outer wells are pushed upward giving rise to a localized state whose energy increases. The shift of the Tamm state upward implies that its distance from the Fermi level changes more slowly than the same distance for the superlattice miniband. Our model calculations show that,

whereas the Fermi level departs from the bottom of the fundamental miniband at a rate of about 12 meV for every 10^{12} cm^{-2} of doping atoms introduced into the InP barriers, the distance from the Fermi level to the Tamm states increases by only 7.3 meV. Thus, the population of the Tamm state is much less sensitive to the doping concentration than the population of the superlattice minibands.

The ratio between the frequencies of magnetoresistance oscillations associated with Tamm and with miniband electrons is roughly independent of the number of wells in the structure, N . However, the relative part of the Tamm electrons in the absolute zero-field conductivity parallel to the layers decreases with N . Since the frequency of oscillation associated with Tamm electrons is about half of the frequency associated with electrons in the bulk of the superlattice, each Tamm state will hold about half the number of electrons accommodated by each of the wells in the bulk. Taking into account that there are two equivalent Tamm states, one for each end of the superlattice, the total amount of electrons in the bulk of the superlattice is about N times

greater than the density of electrons confined at the surfaces. Assuming that electrons in all states have a similar mobility, the surface-localized state will contribute with a fraction $\sim 1/N$ of the total conductivity, which in our samples ($N = 16$) is only about 6%.¹⁷

In summary, we showed that in modulation-doped superlattices densely populated Tamm states arise due to the energy band bending effect. The energy of the Tamm subband can be tuned through the doping density, but its population is relatively insensitive to this parameter. At the doping levels ($\sim 10^{12} \text{ cm}^{-2}$) used in this work, the Tamm states give a major contribution to the SdH spectrum, whose amplitude should decrease with the number of wells in the structure, but whose frequency is independent of N .

ACKNOWLEDGMENTS

This work was supported by the government agencies CNPq, FAPESP, and CAPES.

-
- ¹I. Tamm, *Phys. Z. Sowjetunion* **1**, 733 (1932).
²H. Ohno, E.E. Mendez, J.A. Brum, J.M. Hong, F. Agulló-Rueda, L.L. Chang, and L. Esaki, *Phys. Rev. Lett.* **64**, 2555 (1990).
³F. Agulló-Rueda, E.E. Mendez, H. Ohno, and J.M. Hong, *Phys. Rev. B* **42**, 1470 (1990).
⁴H. Ohno, E.E. Mendez, A. Alexandrou, and J.M. Hong, *Surf. Sci.* **267**, 161 (1992).
⁵T. Miller and T.-C. Chiang, *Phys. Rev. Lett.* **68**, 3339 (1992).
⁶Roger H. Yu, *Phys. Rev. B* **47**, 15 692 (1993).
⁷Roger H. Yu, *Appl. Phys. Lett.* **65**, 1531 (1994).
⁸H.K. Sy and T.C. Chua, *Phys. Rev. B* **48**, 7930 (1993).
⁹H.K. Sy and T. Chua, *Physica B* **194**, 1301 (1994).
¹⁰R. Kucharczyk, M. Stelicka, A. Akjouj, B. Djafari-Rouhani, L. Dobrzynski, and E.H. El Boudouti, *Phys. Rev. B* **58**, 4589 (1998).
¹¹A. Kaczynski, R. Kucharczyk, and M. Stelicka, *Phys. Rev. B* **59**, 4961 (1999).
¹²A.B. Henriques, L.K. Hanamoto, R.F. Oliveira, P.L. Souza, L.C.D. Gonçalves, and B. Yavich, *Physica B* **273**, 835 (1999).
¹³H.L. Störmer, J.P. Eisenstein, A.C. Gossard, W. Wiegmann, and K. Baldwin, *Phys. Rev. Lett.* **56**, 85 (1986).
¹⁴Miniru Kawamura, Akira Endo, Masakatsu Hirasawa, Shingo Katsumoto, and Yasuhiro Iye, *Physica B* **249**, 882 (1998).
¹⁵The parameters used in the calculations are the following: electron effective mass, $m_e^*(\text{InP})=0.08m_0$ and $m_e^*(\text{In}_x\text{Ga}_{1-x}\text{As})=0.045m_0$; conduction band discontinuity, $\Delta E_C=230 \text{ meV}$, and dielectric constant, $\epsilon=11.8$ throughout the structure. The exchange-correlation correction to the confining potential was calculated in the LDA approximation of Hedin and Lundqvist (L. Hedin and B. Lundqvist, *J. Phys. C* **4**, 2064 (1971)).
¹⁶C. Wetzel, A. Efros, A. Moll, B. Meyer, P. Omling, and P. Sobkowicz, *Phys. Rev. B* **45**, 14 052 (1992); D. Schneider, L. Elbrecht, J. Creutzburg, A. Schachetzki, and G. Zwinge, *J. Appl. Phys.* **77**, 2829 (1994).
¹⁷Even though the density of electrons in the Tamm states is much smaller than in the superlattice, in Figs. 1(b) and 1(d), the relative magnitude of the Fourier components appear comparable, which is due to the numerical procedures, outlined in Sec. II, that were used to arrive at the Fourier spectra and which enhanced the Tamm peak [see, for instance, A.B. Henriques, *Phys. Rev. B* **50**, 8658 (1994) for a description of the effects of the numerical procedures upon the Fourier spectra], and also due to the greater quantum mobility of Tamm electrons, which are described by a smaller cyclotron mass.